DOI: 10.1002/adma.200601991

Water-Redispersible Isolated Single-Walled Carbon Nanotubes Fabricated by In Situ Polymerization of Micelles**

By *Tae-Hwan Kim*, *Changwoo Doe*, *Steven R. Kline*, and *Sung-Min Choi**

Single-walled carbon nanotubes (SWNTs) have remarkable mechanical, electrical, and thermal properties[1,2] and have a wide range of potential applications, such as nanoscale electronic devices,[3,4] energy storage,[5,6] and reinforcement for materials.[7,8] In many cases, however, insolubility and bundling of SWNTs in aqueous solution because of their strong hydrophobicity[9,10] and van der Waals attractions,[11] respectively, are problematic for practical applications. Recently there have been many studies on achieving the homogenous dispersion of isolated SWNTs in aqueous solution by using amphiphilic molecules such as surfactants,[12–16] polymers,[17–20] lipids,[21,22] or DNAs[23–25] as dispersants. However, because of the dynamic nature of the self-assembled structures of these amphiphilic molecules the SWNT dispersions are sensitive to changes in external conditions, such as temperature and concentration, and can be destroyed during material processing, forming bundled aggregates and making additional processing very difficult. For example, once surfactant-aided dispersions of isolated SWNTs are freeze-dried they can not be redispersed in water, instead forming aggregates of bundled SWNTs.

Here, we report a new type of noncovalently (i.e., no covalent bonding between the dispersants and the SWNTs) functionalized isolated SWNT powder that is easily dispersible in water by only ten minutes of mild vortex mixing. This was achieved by i) dispersing SWNTs in water by using a cationic surfactant that has polymerizable counterions, and ii) permanently fixing the surfactant monolayer on the SWNTs by in situ free-radical polymerization of the counterions, followed by freeze-drying. To our knowledge, this is the first demonstration of noncovalently functionalized SWNTs that are made readily redispersible in water even after harsh processing such as freeze-drying.

HiPco (high-pressure CO conversion) SWNTs (2 mg mL^{-1}) were mixed in water with the cationic surfactant cetyltrimethylammounium 4-vinylbenzoate (CTVB, 5 mg mL^{-1}), which has polymerizable counterions.[26,27] Super-purified HiPco SWNTs (purity > 98 wt %) were purchased from Carbon Nanotechnologies Inc., and the CTVB molecule was synthesized in-house.[26,27] The mixture of SWNTs and CTVB was sonicated for one hour to exfoliate bundled SWNTs and produce individually isolated SWNTs with an adsorbed layer of CTVB. The CTVB monolayer on the SWNT surface was "locked in" by in situ free-radical polymerization of the counterions of CTVB at 60 °C (by injecting the free-radical initiator 2,2′-azobis[2-(2-imidazolin-2-yl) propane] dihydrochloride (VA-044), Fig. 1). NMR measurements of the polymerized mixture showed that peaks corresponding to vinyl groups were almost completely absent, indicating nearly 100 % polymerization of the counterions (see Supporting Information). To separate the isolated SWNTs from the bundled ones, the polymerized mixture was ultracentrifuged (ca. 111 000 *g*) for 4 h, and the upper ca. 70 % of the solution, which showed homogeneous dispersion of SWNTs, was decanted.[28] The decanted solution contained isolated SWNTs coated with polymerized CTVBs (p-SWNT) and polymerized CTVB micelles (p-CTVB) which were not involved in SWNT coating. To reduce the content of p-CTVB, the decanted mixture was filtered through a membrane with pores of 0.22 μm. The UV-vis-NIR (NIR: near-IR) spectra of the filtered mixture showed sharp van Hove transition peaks (Fig. 2b) that are typical for individually isolated SWNTs in solution.[28] The absorption spectra were also used to estimate the concentration of SWNTs (0.08 mg mL^{-1}) and CTVB (2.6 mg mL^{-1}) in the solution[29,30] after filtering. This p-SWNT dispersion was diluted or concentrated for further characterization.

To test the stability and redispersibility of the p-SWNTs, the decanted and filtered dispersion of p-SWNTs (SWNT 0.13 mg mL^{-1}) was freeze-dried, resulting in a black powder of p-SWNT. The p-SWNT powder was easily dissolved in water at the same concentration as before freeze-drying with only ten minutes of mild vortex mixing. It should be noted that the resulting dispersion of p-SWNTs did not form any visible aggregates, whereas the CTVB-aided dispersion of SWNTs without polymerization (u-SWNT) was not cleanly redis-

[*] Prof. S.-M. Choi, T.-H. Kim, C. Doe
Department of Nuclear and Quantum Engineering
Korea Advanced Institute of Science and Technology
373-1 Guseong-dong, Yuseong-gu
Daejeon 305-701 (Korea)
E-mail: sungmin@kaist.ac.kr
Dr. S. R. Kline
NIST Center for Neutron Research
Gaithersburg, MD 20899-8562 (USA)

[**] T.H.K. and C.D. contributed equally to this work. This work was supported by the Basic Atomic Energy Research Institute (BAERI) Programs and the CNRF project of the Ministry of Science and Technology of Korea. This work utilized facilities supported in part by the National Science Foundation under Agreement No. DMR-9986442. The mention of commercial products does not imply endorsement by NIST, nor does it imply that the materials or equipment identified are necessarily the best available for the purpose. Supporting Information is available online from Wiley InterScience or from the author.

ADVANCED MATERIALS

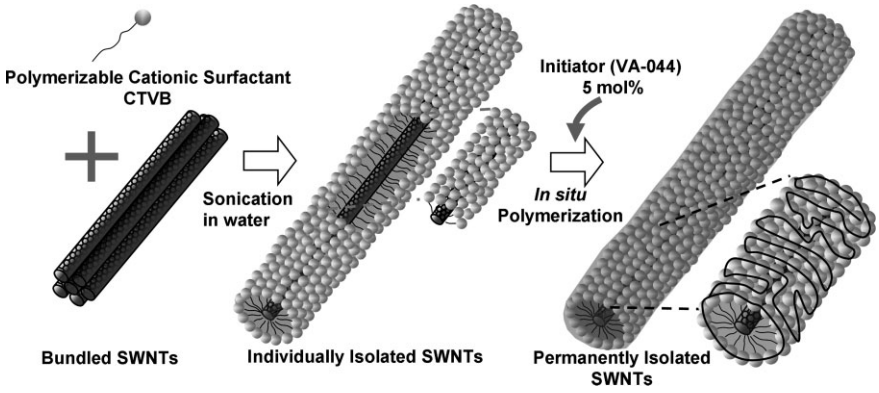

Figure 1. Procedure to make the isolated SWNTs coated with polymerized CTVBs. The in situ free-radical polymerization was performed by injecting 5 mol% (relative to the CTVB concentration) VA-044 initiator at 60 °C.

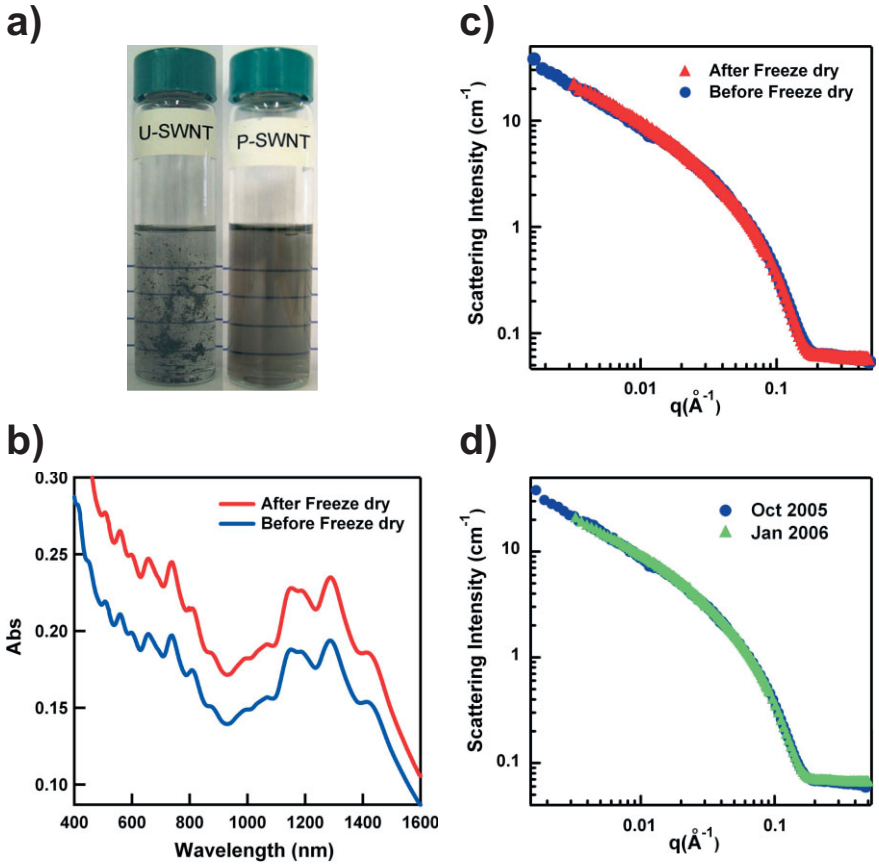

Figure 2. a) Visual comparison of u-SWNTs (left) and p-SWNTs (right) after re-dispersion in water. b) UV-vis-NIR spectra and c) SANS intensities of p-SWNT dispersions in D_2O before and after freeze-drying. The UV-vis-NIR spectrum after freeze-drying was vertically shifted for visual clarity (×1.2). d) SANS intensities of p-SWNT dispersion in D_2O (SWNT 0.13 mg mL^{-1}) after an interval of 3 months. The variable $q = (4\pi/\lambda)\sin(\theta/2)$ represents the magnitude of the scattering vector.

persed in water after freeze-drying, forming aggregates of bundled SWNTs (Fig. 2a). The UV-vis-NIR spectra of p-SWNT dispersions before and after freeze-drying were essentially identical, which indicates the excellent redispersibility of p-SWNTs (Fig. 2b). To compare the microstructures of the p-SWNT dispersions before and after freeze-drying, small-angle neutron scattering (SANS) measurements were performed using the NG7 30 m SANS instrument at the National Institute of Standard and Technology (NIST) in Gaithersburg, MD.[31] All SANS measurements were carried out at 25 °C. As shown in Figure 2c, the SANS intensities of p-SWNT dispersions in D_2O before and after freeze-drying are essentially identical, indicating no change of the microstructure of p-SWNT dispersions. These measurements clearly show that the CTVB coating on SWNT becomes so stable upon polymerization that p-SWNT is readily redispersible in water even after harsh processing such as freeze-drying. The p-SWNT dispersions also showed good long-time stability. The SANS intensities of a p-SWNT dispersion in D_2O (SWNT 0.13 mg mL^{-1}) measured when freshly prepared and then three months after preparation were identical, indicating no structural change of the p-SWNT dispersion within that time interval (Fig. 2d).

Figure 3 shows the SANS intensities of a p-SWNT dispersion in D_2O (SWNT 0.03 mg mL^{-1} and CTVB 1.2 mg mL^{-1}) and a p-CTVB solution in D_2O (1.2 mg mL^{-1}) without SWNTs. It should be noted that in the low q region, where $q = (4\pi/\lambda)\sin(\theta/2)$ is the magnitude of the scattering vector and θ is the scattering angle, the intensity of p-SWNT dispersions do not show $q^{-\alpha}$ ($2 < \alpha < 3$) behavior which is typical for networked SWNTs as found in all the previous SANS studies[32–34] of SWNT dispersions in aqueous solution. In fact, α is 0.94, slightly smaller than 1. If the p-SWNTs are fully dispersed without forming any network, they can be understood as rigid cylindrical particles freely dispersed in water, and their SANS intensity should show q^{-1} behavior in the low q region. However, some amount of p-CTVB, which has a flattened SANS intensity in the low q region (green circles in Fig. 3), still exists in the p-SWNT dispersion. To a first approximation, the contribution of remaining p-CTVBs can be

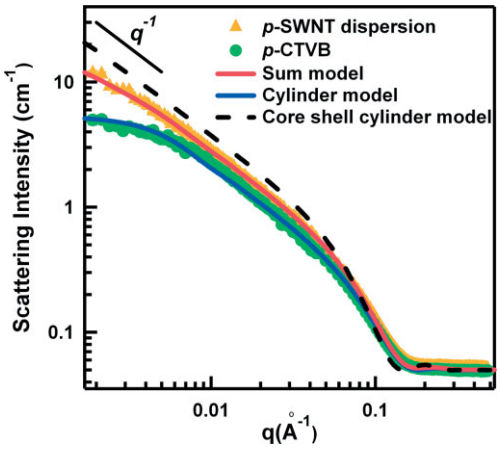

Figure 3. SANS intensities and model calculations of a p-SWNT dispersion and p-CTVB in D_2O.

added to the q^{-1} behavior of p-SWNT (dotted line in Fig. 3) making α slightly less than one. Even at higher p-SWNT concentrations (SWNT 0.5 mg mL^{-1}), α was 0.95, still slightly less than one. This clearly indicates that the p-SWNTs are well-dispersed in a purely isolated way without forming any network.

Several different models have been suggested for the microstructures of surfactant layer on SWNTs, which include the cylindrical encapsulation model,[28,30] the hemimicellar model,[21,22] and the random adsorption model.[16] Currently, the final resolution among the models has not been achieved and the surfactant adsorption structures may strongly depend on the physical characteristics and geometrical properties of the surfactants.[21] To understand the microstructure of the polymerized surfactant layer on SWNTs we simulated the scattering intensity of a p-SWNT dispersion by using a sum of two models, a core/shell cylindrical form factor and a cylindrical form factor, to describe the p-SWNT and p-CTVB, respectively. In the hemimicellar striation model a peak in q-space, originating from the periodic correlation between the hemimicellar striations, is expected.[22] All the SANS intensities measured in this study, however, did not show any indication of the correlation peak at $q = 2\pi/40$ Å^{-1} = 0.157 Å^{-1}. Therefore, we did not consider the hemimicellar model in this analysis. The neutron scattering length densities for SWNT, CTVB, and D_2O are 4.9×10^{-6}, 3.5×10^{-7}, and 6.33×10^{-6} Å^{-2}, respectively. Because the dispersions are very dilute, interparticle interactions were not considered. The SANS intensity of the p-CTVB alone in D_2O (green circles in Fig. 3) was analyzed to determine the p-CTVB cylinder dimensions, which were a radius and length of 2.0 nm and 70 nm, respectively. When modeling the mixture, these values were held fixed for the p-CTVB. To represent the coated p-SWNTs, the core radius, shell thickness, and length of the core/shell cylinder were set to be 0.5 nm (radius of a typical SWNT), 2.0 nm (radius of the cylindrical p-CTVB micelle), and 500 nm (estimated from atomic force microscopy (AFM) images), respectively. In this simulation the volume fractions $\varphi_{\text{p-CTVB}}$ and $\varphi_{\text{p-SWNT}}$ were adjusted to match the SANS intensity. It should be noted that the summed model (red solid line) with $\varphi_{\text{p-SWNT}} = 0.00082$ and $\varphi_{\text{p-CTVB}} = 0.001$ agrees well with the SANS intensity of the p-SWNT dispersion. To test the random adsorption model, we simulated the SANS intensities with a shell thickness of 1–1.5 nm (the expected thickness of the shell if surfactants were randomly adsorbed on SWNTs), which did not match with the measured SANS intensities. These results indicate that the cylindrical encapsulation model is relevant for the p-SWNTs. When a closely packed cylindrical monolayer of CTVB on SWNT is assumed, as illustrated in Figure 1, and the head group area of CTVB (66 Å^2)[26,27] is used, the number of CTVB molecules adsorbed per unit length of SWNT is calculated to be 24 nm^{-1}.

The diameter distributions of bare SWNTs (obtained by burning p-SWNTs) and p-SWNTs were determined from the AFM measurements, as shown in Figure 4. The diameter distribution of bare SWNTs is peaked at (1 ± 0.1) nm, and diameters less than 2 nm occupy 90 % of the distribution which indicates that p-SWNTs are dispersed in an isolated form. The diameter distribution of p-SWNTs is peaked at (5 ± 0.1) nm, and 86 % of the distribution is in the range of 4.4–5.6 nm. The polymerized surfactant shell thickness of the p-SWNTs, which is determined from the diameter distributions, is about 2 nm. This result is consistent with the SANS analysis and further supports the cylindrical encapsulation model for the p-SWNTs.

The redispersibility of p-SWNTs was tested for an organic solvent: ethanol. The freeze-dried p-SWNTs were completely redispersed in ethanol by only ten minutes of vortex mixing. The UV-vis-NIR spectrum of p-SWNTs redispersed in ethanol was essentially identical to that of p-SWNTs dispersed in water. This clearly indicates that the encapsulation of SWNTs by polymerized CTVB is very stable even in ethanol. The details of the redispersibility of p-SWNTs in various organic solvents will be presented in a forthcoming publication.

In summary, we have successfully developed noncovalently functionalized and individually isolated SWNTs that are readily redispersible in water, even after freeze-drying, and are stable for months. Unlike the previous SWNT dispersions, the p-SWNTs do not form any aggregates or networks at the concentrations investigated in this study. These properties of the p-SWNTs make it possible to prepare highly controlled dispersions of SWNTs in water and allow for further processing in various practical applications.

Experimental

Cetyltrimethylammonium hydroxide (CTAOH) and 4-vinylbenzoic acid (VBA) were purchased from Aldrich. The water-soluble free-radical initiator VA-044 was purchased from Wako Chemicals. D_2O (99.9 mol % deuterium enriched) was purchased from Cambridge Isotope Laboratories. Super-purified HiPco single-walled carbon nanotubes (purity > 98 wt %) were purchased from Carbon Nanotechnologies Inc. H_2O was purified with a Millipore Direct Q system immediately before use. Cetyltrimethylammonium 4-vinylbenzoate (CTVB) was synthesized by neutralization of VBA in the presence of

ADVANCED MATERIALS

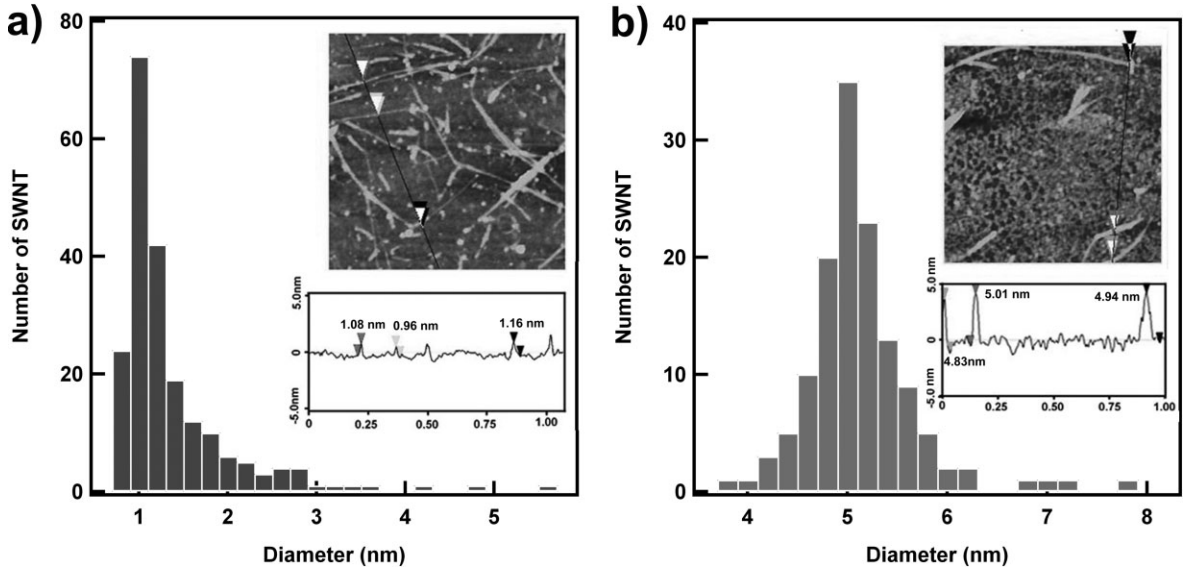

Figure 4. The diameter distributions of a) the bare SWNTs and b) p-SWNTs. The insets are AFM images (1 μm × 1 μm) and sectional analyses of a) bare SWNTs and b) p-SWNTs.

a slight stoichiometric excess of CTAOH, followed by repeated crystallization. The detailed procedure has been described elsewhere [26,27].

UV-vis-NIR measurements were performed by using a Jasco V-570 model spectrometer and 2 mm path length quartz cells in D_2O at room temperature. The concentration of CTVB and SWNTs in the p-SWNT dispersion was quantified by UV-vis-NIR measurements [29,30]. To estimate the actual concentration of SWNTs and CTVB in the p-SWNT dispersion, we prepared reference solutions of SWNT ultrasonicated for 1 h and CTVB alone at known concentration in the range of 0.001–0.02 mg mL^{-1} and 0.03–0.3 mg mL^{-1}, respectively. The absorbance of the reference solution of SWNT and CTVB was increased linearly with the concentration of SWNT and CTVB. The absorption peaks of CTVB and SWNT in the p-SWNT dispersion were compared to those of the reference solutions at 230 nm and 744 nm, respectively.

The AFM images were taken in tapping mode by using a VEECO AFM instrument (Nanoman, SECPM). For the AFM measurements, a p-SWNT dispersion was spin-coated (at 4000 rpm for 1.5 min) onto silicon wafers. To prepare the sample for bare SWNT, a p-SWNT dispersion deposited onto a silicon wafer by spin-coating was burned for 4 h at 330 °C to remove the CTVB absorbed on SWNT.

Small-angle neutron scattering (SANS) measurements were performed to characterize the structures of the p-SWNT samples. SANS experiments were carried out on the NG7 30 m SANS instrument at the National Institute of Standard and Technology (NIST) in Gaithersburg, MD [31]. Neutrons of wavelength $\lambda = 6$ Å and 8.1 Å with full width at half-maximum $\Delta\lambda/\lambda = 11$ % were used. Three different sample-to-detector distances (SDD = 1.1 m and 13.5 m for $\lambda = 6$ Å, and SDD = 15.3 m for $\lambda = 8.1$ Å) were used to cover the overall q range of 0.0015 Å$^{-1} < q < 0.5368$ Å^{-1}. To extend the low q limit, we used a set of refractive focusing lenses [35] for $\lambda = 8.1$ Å and SDD = 15.3 m. Sample scattering was corrected for background and empty cell scattering, and the sensitivity of individual detector pixels. The corrected data sets were placed on an absolute scale by using data reduction software provided by NIST [36] through the direct beam flux method. All SANS measurements were carried out in D_2O at 25 °C.

Received: September 1, 2006
Revised: October 20, 2006
Published online: March 12, 2007

[1] R. Saito, G. Dresselhaus, M. S. Dresselhaus, *Physical Properties of Carbon Nanotubes*, Imperial College Press, London **1998**.
[2] *Carbon Nanotubes Synthesis, Structure, Properties, and Applications* (Eds: M. S. Dresselhaus, G. Dresselhaus, P. Avouris), Springer, New York **2003**.
[3] S. J. Tans, A. R. M. Verschueren, C. Dekker, *Nature* **1998**, *393*, 49.
[4] C. Zou, J. Kong, E. Yenilmez, H. Dai, *Science* **2000**, *290*, 1552.
[5] K. H. An, W. S. Kim, Y. S. Park, Y. C. Choi, S. M. Lee, D. C. Chung, D. J. Bae, S. C. Lim, Y. H. Lee, *Adv. Mater.* **2001**, *13*, 497.
[6] R. H. Baughman, A. A. Zakhidov, W. A. de Heer, *Science* **2002**, *297*, 787.
[7] J. N. Coleman, U. Khan, Y. K. Gun'ko, *Adv. Mater.* **2006**, *18*, 689.
[8] P. M. Ajayan, L. S. Schadler, C. Giannaris, A. Rubio, *Adv. Mater.* **2000**, *12*, 750.
[9] J. Hilding, E. A. Grulke, Z. G. Zhang, F. Lockwood, *J. Dispersion Sci. Technol.* **2003**, *24*, 1.
[10] M. J. O'Connell, P. Boul, L. M. Ericson, C. Huffman, Y. Wang, E. Haroz, C. Kuper, J. Tour, K. D. Ausman, R. E. Smalley, *Chem. Phys. Lett.* **2001**, *342*, 265.
[11] L. A. Girifalco, M. Hodak, R. S. Lee, *Phys. Rev. B: Condens. Matter Mater. Phys.* **2000**, *62*, 13 104.
[12] D. Tasis, N. Tagmatarchis, V. Georgakilas, M. Prato, *Chem. Eur. J.* **2003**, *9*, 4000.
[13] M. F. Islam, E. Rojas, D. M. Bergey, A. T. Johnson, A. G. Yodh, *Nano Lett.* **2003**, *3*, 269.
[14] V. C. Moore, M. S. Strano, E. H. Haroz, R. H. Hauge, R. E. Smalley, *Nano Lett.* **2003**, *3*, 1379.
[15] O. Matarredona, H. Rhoads, Z. Li, J. H. Harwell, L. Balzano, D. E. Resasco, *J. Phys. Chem. B* **2003**, *107*, 13 357.
[16] K. Yurekli, C. A. Mitchell, R. Krishnamoorti, *J. Am. Chem. Soc.* **2004**, *126*, 9902.
[17] B. Z. Tang, H. Xu, *Macromolecules* **1999**, *32*, 2569.
[18] G. R. Dieckmann, A. B. Dalton, P. A. Johnson, J. Razal, J. Chen, G. M. Giordano, E. Munoz, I. H. Musselman, R. H. Baughman, R. K. Draper, *J. Am. Chem. Soc.* **2003**, *125*, 1770.
[19] R. Bandyopadhyaya, E. Nativ-Roth, O. Regev, R. Yerushalmi-Rozen, *Nano Lett.* **2002**, *2*, 25.
[20] O. Regev, P. N. B. ElKati, J. Loos, C. E. Koning, *Adv. Mater.* **2004**, *16*, 248.

[21] Y. Wu, J. S. Hudson, Q. Lu, J. M. Moore, A. S. Mount, A. M. Rao, E. Alexov, P. C. Ke, *J. Phys. Chem. B* **2006**, *110*, 2475.
[22] C. Richard, F. Balavoine, P. Schultz, T. W. Ebbesen, C. Mioskowski, *Science* **2003**, *300*, 775.
[23] M. Zheng, A. Jagota, M. S. Strano, A. P. Santos, P. Barone, S. G. Chou, B. A. Diner, M. S. Dresselhaus, R. S. Mclean, G. B. Onoa, G. G. Samsonidze, E. D. Semke, M. Usrey, D. J. Walls, *Science* **2003**, *302*, 1545.
[24] M. Zheng, A. Jagota, E. D. Semke, B. A. Diner, R. S. Mclean, S. R. Lustig, R. E. Richardson, N. G. Tassi, *Nat. Mater.* **2003**, *2*, 338.
[25] S. Badaire, C. Zakri, M. Maugey, A. Derré, J. N. Barisci, G. Wallace, P. Poulin, *Adv. Mater.* **2005**, *17*, 1673.
[26] S. R. Kline, *Langmuir* **1999**, *15*, 2726.
[27] T. H. Kim, S. M. Choi, S. R. Kline, *Langmuir* **2006**, *22*, 2844.
[28] M. J. O'Connell, S. M. Bachilo, C. B. Huffman, V. C. Moore, M. S. Strano, E. H. Haroz, K. L. Rialon, P. J. Boul, W. H. Noon, C. Kittrell, J. Ma, R. H. Hauge, R. B. Weisman, R. E. Smalley, *Science* **2002**, *297*, 593.
[29] W. Wenseleers, I. I. Vlasov, E. Goovaerts, E. D. Obraztsova, A. S. Lobach, A. Bouwen, *Adv. Funct. Mater.* **2004**, *14*, 1105.
[30] O. Matarredona, H. Rhoads, Z. Li, J. H. Harwell, L. Balzano, D. E. Resasco, *J. Phys. Chem. B* **2003**, *107*, 13 357.
[31] C. J. Glinka, J. G. Barker, B. Hammouda, S. Krueger, J. J. Moyer, W. J. Orts, *J. Appl. Crystallogr.* **1998**, *31*, 430.
[32] W. Zhou, M. F. Islam, H. Wang, D. L. Ho, A. G. Yodh, K. I. Winey, J. E. Fischer, *Chem. Phys. Lett.* **2004**, *384*, 185.
[33] B. J. Bauer, E. K. Hobbie, M. L. Becker, *Macromolecules* **2006**, *39*, 2637.
[34] H. Wang, W. Zhou, D. L. Ho, K. I. Winey, J. E. Fischer, C. J. Glinka, E. K. Hobbie, *Nano Lett.* **2004**, *4*, 1789.
[35] S. M. Choi, J. G. Barker, C. J. Glinka, H. T. Cheng, P. L. Gammel, *J. Appl. Crystallogr.* **2000**, *33*, 792.
[36] NIST SANS Data Reduction and Imaging Software, 2003.

